MOLECULAR ECOLOGY

Molecular Ecology (2017) **26**, 1818–1831 doi: 10.1111/mec.13895

MICROBIAL LOCAL ADAPTATION

Experimental evolution of rhizobia may lead to either extra- or intracellular symbiotic adaptation depending on the selection regime

MARTA MARCHETTI,* CAMILLE CLERISSI,*† ‡ YASMINE YOUSFI,* CARINE GRIS,* OLIVIER BOUCHEZ,§¶ EDUARDO ROCHA,† ‡ STÉPHANE CRUVEILLER,** ALAIN JAUNEAU,† † DELPHINE CAPELA* and CATHERINE MASSON-BOIVIN*

*LIPM, Université de Toulouse, INRA, CNRS, 31326 Castanet-Tolosan Cedex, France, †Microbial Evolutionary Genomics, Institut Pasteur, 25-28 rue Dr Roux, 75015 Paris, France, ‡CNRS, UMR3525, 25-28 rue Dr Roux, 75015, Paris, France, §GeT-PlaGe, INRA, 31326, Castanet-Tolosan Cedex, France, ¶GenPhySE, Université de Toulouse, INRA, INPT, ENVT, 31326 Castanet-Tolosan Cedex, France, **CNRS-UMR8030 and Commissariat à l'Energie Atomique CEA/DSV/IG/Genoscope LABGeM, 2 rue gaston Crémieux, 91057 Evry, France, ††Fédération de Recherches Agrobiosciences, Interactions, Biodiversity, Plateforme d'Imagerie TRI, CNRS, UPS, 31326 Castanet-Tolosan Cedex, France*

Abstract

Experimental evolution is a powerful approach to study the process of adaptation to new environments, including the colonization of eukaryotic hosts. Facultative endosymbionts, including pathogens and mutualists, face changing and spatially structured environments during the symbiotic process, which impose diverse selection pressures. Here, we provide evidence that different selection regimes, involving different times spent in the plant environment, can result in either intra- or extracellular symbiotic adaptations. In previous work, we introduced the symbiotic plasmid of *Cupriavidus taiwanensis*, the rhizobial symbiont of *Mimosa pudica*, into the phytopathogen *Ralstonia solanacearum* and selected three variants able to form root nodules on *M. pudica*, two (CBM212 and CBM349) being able to rudimentarily infect nodule cells and the third one (CBM356) only capable of extracellular infection of nodules. Each nodulating ancestor was further challenged to evolve using serial ex planta–in planta cycles of either 21 (three short-cycle lineages) or 42 days (three long-cycle lineages). In this study, we compared the phenotype of the 18 final evolved clones. Evolution through short and long cycles resulted in similar adaptive paths on lineages deriving from the two intracellularly infectious ancestors, CBM212 and CBM349. In contrast, only short cycles allowed a stable acquisition of intracellular infection in lineages deriving from the extracellularly infecting ancestor, CBM356. Long cycles, instead, favoured improvement of extracellular infection. Our work highlights the importance of the selection regime in shaping desired traits during host-mediated selection experiments.

Keywords: experimental evolution, extracellular, intracellular, rhizobium, symbiosis

Received 5 July 2016; revision received 11 October 2016; accepted 18 October 2016

Introduction

Experimental evolution coupled to resequencing experiments is a powerful approach to provide a comprehensive view of genomic changes of micro-organisms in response to changing environmental conditions and to study the process of adaptation (Elena & Lenski 2003) (Buckling *et al.* 2009; Brockhurst *et al.* 2011; Long *et al.* 2015). Bacteria are ideally suited for such approaches, because they have large populations, short generation times, small genomes that can be easily (re)sequenced and most importantly ancestral and intermediate forms can be frozen as 'fossil records', allowing evaluating

Correspondence: Catherine Masson-Boivin, Fax: +33 561285061; E-mail: catherine.masson@toulouse.inra.fr

adaptation to the new environment by comparing the performance of evolved individuals to ancestors.

Experimental evolution has been predominantly used to study genetic adaptation to very simple and homogenous culture conditions, providing essential lessons on general evolutionary processes (Barrick *et al.* 2009; MacLean *et al.* 2010). Experimental evolution has also recently been used to tackle challenging complex questions such as the evolution of biotic interactions (Brockhurst & Koskella 2013), including virus–bacteria co-evolution (Paterson *et al.* 2010; Scanlan *et al.* 2011), adaptation of pathogens to human (Yang *et al.* 2011) and plant (Guidot *et al.* 2014) environments, and insect–bacteria mutualism (Chrostek & Teixeira 2015). Whereas culture in synthetic media results in constant selection pressure, biotic interactions impose diverse selective pressures in terms of competition for host resources and host immunity (Jackson *et al.* 2011), and actual forces and mechanisms driving microbe traits are difficult to assess a priori. Moreover endosymbionts, including pathogens and mutualists, are typically confronted to changing and spatially structured environments, being able to thrive in different cell types and tissues and to cope with the multiple host responses encountered during the symbiotic process. In all cases, the experimental design is crucial as it may impact the competitive advantage one genotype has over another and thus results in evolutionary pathways that may produce either gains or losses in fitness.

The rhizobium–legume symbiosis is a model system to study species interaction as a driving force of adaptive evolution. Rhizobia have evolved the environmental essential function of fixing atmospheric nitrogen in symbiosis with legumes (Masson-Boivin *et al.* 2009). They are facultative symbionts able to switch from a free-living saprophytic state to an endosymbiotic life when they encounter a compatible host. The symbiotic process is complex and involves many stages including rhizoplane colonization, root entry, nodule organogenesis, nodule cell infection and persistence and nitrogen fixation (Gibson *et al.* 2008; Oldroyd *et al.* 2011). Ultimately, nodules senesce and bacteria are released to the soil where they compete with other bacteria for survival and colonization of a new host.

Most rhizobia arose via horizontal gene transfer (HGT) of a set of key symbiotic genes, the nodulation and nitrogen fixation genes located on mobile elements, converting soil bacteria into facultative mutualistic symbionts of legumes (Sullivan *et al.* 1995). Rhizobia belong to at least 14 different saprophytic and pathogenic genera of α- and β-proteobacteria, indicating that transfer over large phylogenetic distances successfully occurred several times during evolution (Remigi *et al.* 2016). Yet, in the laboratory and likely *in natura*, transfer in itself is usually unproductive between evolutionary distant taxa (Hirsch *et al.* 1984; Marchetti *et al.* 2010). The ecological success of long-range transfer may thus require further adaptations of the recipient bacteria to achieve symbiosis (Tian *et al.* 2012). The successive fixation of beneficial mutations arising in large soil/rhizospheric populations is ensured by rounds of strong selection at the root entry stage followed by clonal amplification within nodules and ultimate release of bacteria in the soil (Remigi *et al.* 2014). Unravelling the mechanisms and forces that drive endosymbiotic adaptation is crucial for understanding the emergence of bacterial symbiosis with legumes and transfer to nonlegume crops (Charpentier & Oldroyd 2010).

To replay the HGT-driven evolution of a new rhizobial genus, we introduced the pRalta symbiotic plasmid of the *Mimosa* symbiont *Cupriavidus taiwanensis* into the phytopathogen *Ralstonia solanacearum* GMI1000, generating a non-nodulating chimera. *Mimosa pudica* was used as a trap to first select three nodulating variants of the *Ralstonia* chimera (selection cycle). Two of them, CBM212 and CBM349, acquired rudimentary nodule cell (intracellular) infection capacity concomitantly to nodulation, while the third one, CBM356, induced nodules that were only extracellularly infected, that is colonized in the intercellular spaces (referred as to extra- or intercellular infection) (Marchetti *et al.* 2010) (Fig. S1, Supporting information). Six independent lineages were then evolved from each nodulating variant using sixteen serial ex planta–in planta cycles of either 21 days or 42 days, generating three SC (for short cycles) lineages and three LC (for long cycles) lineages per ancestor (Fig. S1, Supporting information). Two different selection regimes were used in parallel as we hypothesized that short cycles would select for improved nodulation and infectivity while long cycles would also select for increased persistence, that is extended intracellular life, of nodule bacteria. Previous analysis of short lineages showed that evolution was very fast. Nodulation and intracellular infection of nodule cells were indeed dramatically improved over 16 cycles (~400 generations) in the nine SC parallel lineages (Guan *et al.* 2013; Marchetti *et al.* 2014). The rapidity of the *Ralstonia* evolution was due to combined effects of the experimental setting that favours the selection of the most efficiently nodulating and infecting clones in each cycle, and the presence of an *imuABC* mutagenesis cassette on the acquired symbiotic plasmid, which transiently elevates the mutation rate of the recipient genome in the rhizosphere creating a burst in genetic diversity favourable for evolution (Remigi *et al.* 2014).

Here, we provide evidence that the selection regime impacts on the outcome of the endosymbiotic adaptation of chimeric *Ralstonia* during laboratory evolution.

We analysed the final clones derived from the nine LC lineages and compared their phenotype and the number of mutational events on their genome to that of the final clones derived from the nine SC lineages (Marchetti *et al.* 2014). Although short and long cycles resulted in similar levels of adaptation in lineages deriving from the two rudimentary intracellularly infectious ancestors, long cycles, in contrast to short cycles, did not allow a stable acquisition of nodule cell infection in lineages deriving from the extracellularly infecting ancestor. Analysis of such a lineage revealed that an adaptive mutation for intracellular infection was acquired and fixed, but its effect was countered by additional genome modification(s). Moreover, long selection regime resulted in more time spent in stressful ex planta conditions with concomitant accumulation of 50% more mutations. This complicates even more the analysis of the genetic basis of adaptation.

Materials and methods

Bacterial strains and growth conditions

Bacterial strains and plasmids used in this work are listed in Table S3 (Supporting information). *Ralstonia solanacearum* strains were grown at 28 °C on B medium supplemented with 28 mM glucose (BG), B medium or minimal medium (MM) supplemented with 2% glycerol for bacterial transformation (Sigma-Aldrich, St. Louis, MO, USA) (Boucher *et al.* 1985). *Cupriavidus taiwanensis* strains were grown at 28 °C on TY medium supplemented with 6 mM $CaCl_2$. Antibiotics were used at the following concentrations (in micrograms per millilitre): trimethoprim 100, tetracycline 10, gentamicin 10, chloramphenicol 12.5, kanamycin 50 and streptomycin 600.

Generation of symbiotically evolved clones and populations

Long lineages (LC, 42-day cycles) were evolved in parallel to short lineages (SC, 21-day cycles), as previously described in Marchetti *et al.* (2014), except that we used ex planta–in planta cycles of 42 days instead of 21 days. Briefly, the ancestral strains CBM212, CBM349 and CBM356 grown overnight in BG medium supplemented with trimethoprim were each inoculated to three sets of 20 *Mimosa pudica* plants (two plants per tube). *Ca.* 10^7 bacteria per tube were used as inoculum. Forty-two days after inoculation, all nodules from each set of 20 plants were pooled, sterilized with 2.6% sodium hypochlorite during 15 min and crushed. About 10% of the nodule crush was used to inoculate on the same day a new set of 20 plants, except in cycle 4 of lineage L, where plants were inoculated with a 48-h culture of nodule crush obtained in the previous cycle. Indeed, very few nodules could be recovered in cycle L4, and bacteria collected from the nodule crush were probably insufficient to inoculate a new set of 20 plants. At each cycle, serial dilutions of each nodule crush were plated and one clone was randomly selected from the highest dilution and purified. The selected clones, the rest of the nodule crushes and a 48-h culture of bacteria from an aliquot of nodule crushes were stored at −80 °C. All the in planta phenotypic analyses were performed using the purified clone.

During evolution of lines, the mean time bacteria spent ex planta or in planta was estimated using nodulation kinetics of nine final clones and the three ancestors, as previously described (Remigi *et al.* 2014). We first calculated the time when half of the nodules obtained at 21 dpi (days post-inoculation) or 42 dpi appeared. To estimate the mean ex planta time, we subtracted 3 days (estimated time between the moment bacteria enter and the moment the nodule is visible). To estimate the mean in planta time, we subtracted the ex planta mean time from the incubation time, 21 or 42.

Strain construction

For competition experiments, the GFP- or mCherry-expressing strains were constructed by integration of the reporter gene in the chromosome downstream from *glmS* using the pRC delivery system as previously described (Monteiro *et al.* 2012). To this end, the pRCK-Pps-GFP or pRCK-Pps-mCherry plasmid carrying the P*psbA* promoter region upstream the GFP or the mCherry gene were cloned into the pRCK-Pps plasmid and transformants were obtained by natural transformation as described for strain GMI1000 (Boucher *et al.* 1985). Briefly, recipient bacteria were grown for 1–2 days in MM supplemented with 2% glycerol (Sigma-Aldrich) and 100 μL of the culture was then mixed with approximately 2 μg of plasmid linearized with the restriction enzyme *SfI*. The resulting suspension was then applied on the surface of a B medium agar plate (Boucher *et al.* 1985). After incubation at 28 °C for 1 or 2 days, bacteria were resuspended in 500 μL of B medium and 100 μL was plated on B-solid medium containing the appropriate antibiotics to select for transformants.

For mutant construction, the point mutations *hrpG*A179V were introduced in the genome of the CBM356 strain using the MuGENT technique as described by Dalia *et al.* (2014). Briefly, this technique is based on the natural competence of bacteria and the frequency of cotransformation of two unlinked DNA fragments, one fragment carrying an antibiotic resistance marker for selection of transformants and one PCR

product carrying the point mutation. The selected DNA marker used was the *Sfi*I-linearized pRCK-Pps-GFP plasmid that allows the chromosomal integration of the kanamycin resistance gene and the constitutive P*psbA*-GFP fusion at the *glmS* intergenic region (Monteiro *et al.* 2012). The unselected DNA fragment was obtained by PCR amplification of about 6-kb region surrounding the mutation position using genomic DNA as template and high-fidelity Phusion polymerase (Roche) using the primers oCBM2893 and oCBM2894 (Table S4, Supporting information). The PCR product was precipitated with 1/10 volume of sodium acetate 3 M and two volumes of ethanol and resuspended in 30 μL of water. Bacteria were transformed with 1.5 μg of PCR products and 300 ng of marked DNA. Transformants were selected on kanamycin and screened by sequencing after PCR amplification of a region containing the SNP using the primers oCBM622 and oCBM625 (Table S4, Supporting information).

To check the role of original pRalta on R16 phenotype, exchange of evolved pRalta of the R16 clone by the original pRalta was achieved as previously described (Marchetti *et al.* 2014). Briefly, replacement was realized by conjugation of R16 with the donor *C. taiwanensis* CBM61 strain carrying the symbiotic plasmid pRalta::Tn5-B13S (tetracycline resistant) and the helper plasmid RP4-7. Transconjugants resistant to tetracycline and sensitive to trimethoprim were purified and then transformed with the pMG02 plasmid to exchange the Tn5-B13S by the trimethoprim cassette as described (Marchetti *et al.* 2014). Transformants were verified by sequencing of the PCR product containing the specific SNP of the *hrpG* gene present in R16 (oCBM622 and oCBM625 primers). The replacement of the pRalta was confirmed by the loss of a specific SNP present in the evolved pRalta of the R16 clone (oCBM2988 and oCBM2990 primers) after sequencing (Table S4, Supporting information).

Plant assays and cytological analysis

Two lots of *M. pudica* seeds, one collected in Thailand fields and the other in Australia fields, were purchased from B&T World Seed (Paguignan, France). Thailand seeds were used for experimental evolution and Australian seeds for all phenotypic analyses. Seedlings of *M. pudica* were grown in Gibson tubes under N-free conditions as previously described (Marchetti *et al.* 2010; Guan *et al.* 2013).

For cytology, nodules were harvested at 21 dpi and cut into 55-μm sections with a Leica VT1000S vibratome apparatus. For each nodule, the largest longitudinal section was observed using an inverted microscope (DMIRBE; Leica) and images acquired using a CCD camera (Color Coolview, Photonic Science, Milham, UK). Semiquantitative analysis of infection and necrosis was performed on sections of nodules induced by *C. taiwanensis*, *C. taiwanensis nifH*, ancestral and evolved clones as previously described (Marchetti *et al.* 2014). Briefly, the infection zone inside the nodule section was manually delimitated and infection or necrosis area measured using the IMAGE-PRO PLUS software based on the hue, saturation and intensity (HIS) method that allows delimiting and measuring these areas on a colour basis (Marchetti *et al.* 2014) (Media Cybernetics, Rockville, MD, USA). Surfaces are measured in pixels. For each nodule section, the infection/necrosis surface was calculated as a percentage of the total nodule surface. Extracellular quantification was performed on sections of nodules induced by bacteria expressing a constitutive *lacZ* fusion as present in the ancestral chimera after staining with X-Gal following the standard procedure as described (Marchetti *et al.* 2010). In this case, infection was measured by quantifying the blue staining of the manually delimitated total nodule section area. Results were obtained from six to 48 nodules and two or three independent experiments.

For persistence analysis, nodules from two plants were recovered at 21 dpi, surface-sterilized and crushed. Nodule crushes were filtered first through a 50-μm filter (CellTrics, Sysmex) and then a 10-μm filter (CellTrics; Sysmex) to eliminate plant tissue residues. Recovered bacteria were incubated for 15 min in live/dead staining solution (5 μM SYTO9 and 30 μM PI in 50 mM Tris [pH 7.0] buffer) (Live/Dead BacLight; Invitrogen, Carlsbad, CA, USA) and analysed with a Sysmex cytometer for live (Syto9 staining) and dead (PI staining) bacterial quantification. Results are reported as percentage of Syto9-stained bacteria of the total bacterial population. Three independent repetitions with 15–20 nodules for each clone were realized except for R16 for which six nodules were analysed.

For competition experiments, tubes containing two plants were co-inoculated with a pair of labelled strains at a 1/1 ratio (10^5 cells/strain). Ancestral and evolved strains were labelled with GFP or mCherry reporter genes, respectively, and bacterial counting was performed using a fluorescent stereo zoom microscope (Axiozoom V16, Zeiss). No transformant could be obtained for J16. In this case, the number of J16 was deducted from the total number of bacteria and the number of ancestral GFP-labelled ancestral strains. For quantification of relative fitness in the plant culture medium, 1 mL of Jensen medium was recovered from the plant tube at 7 dpi and serial dilutions were plated for colony counting. For quantification of the relative fitness on the rhizoplane, roots of each tube were recovered at 7 dpi and vortexed 2 min into water to recover

root-attached bacteria and dilutions were plated for colony counting. Three repetitions were realized with two plants for plant culture medium and rhizoplane relative fitness. For quantification of the relative in planta fitness, nodules from 20 plants were harvested 21 days after inoculation, pooled, surface-sterilized and crushed. Dilutions of nodule crushes were plated on selective solid medium. In all competition experiments, the number of bacteria recovered from nodules was normalized by the inoculum ratio, as following: percentage of bacteria in nodule crush divided by the percentage of bacteria in the inoculum. We confirmed that the two fluorophores have no influence on relative fitness, by performing competition experiments with isogenic CBM212-GFP and CBM212-mCherry strains.

For fitness measurement, plants were inoculated with *C. taiwanensis* wild type, its *nifH* mutant or evolved clones and nodules from six plants were harvested at 21 days after inoculation, pooled, surface-sterilized, crushed and dilutions plated on BG medium to count the number of viable bacteria per nodule as previously described (Marchetti *et al.* 2010). For each strain, three repetitions of fitness measurement were performed.

Genomic analyses

Bacterial clones were sequenced by the GeT platform (http://get.genotoul.fr/) using the Illumina HiSeq2000 technology (mean coverage ~ 400×). High-throughput sequencing data were analysed using the PALOMA bioinformatic pipeline such as described in Remigi *et al.* (2014). To filter sequencing errors or undetected events in ancestors, we did not consider mutations with a score of SNPs/indels (high-quality reads on the position/total reads on the position) <0.4 and an allele ratio (mutated reads on the position/total reads on the position) <0.61. For each clone, estimations of the number of SNPs, indels, synonymous, nonsynonymous, genic, intergenic, transition and transversion were performed on the filtered data sets of mutational events.

Statistical analysis

Pairs of clones were compared for infection and necrosis sizes using the R software (R v. 2.15.2) and the nonparametric statistical test of Kruskal–Wallis combined with a pairwise comparison using Wilcoxon rank-sum test and Bonferroni *P* value adjustment method with a value threshold of 0.05. For fitness and persistence analysis, Student's *t*-test was applied with a threshold of 0.05. For competition experiment, the normalized relative proportions of bacteria were first transformed using the angular transformation (arcsin(sqrt(x)) to normalize their statistical distribution. Next, to compare couples of strains, an analysis of variance was performed on the differences between their transformed proportions (number of replicates = 3). A difference was considered as significant when the corresponding parameter in the ANOVA was significantly different from 0 ($\alpha < 0.05$). All the other statistical analyses were computed using R v.3.1.3 (http://www.R-project.org). Groups of SC and LC clones were compared for phenotypic variables and mutations using the Student's *t*-test (t.test function, {stats} package) (when normality was not rejected (shapiro.test, {stats}), or when the number of observation was lower than 6), or the nonparametric Wilcoxon rank-sum test (wilcox.test, {stats}). Benjamini–Hochberg correction was applied for significance of all multiple comparisons (p.adjust, {stats}). To evaluate whether selective pressures influenced the mutational profile, dN/dS (nonsynonymous to synonymous substitution rate) and dI/dS (intergenic to synonymous substitution rate) ratios were compared to simulations of genome evolution. First, the number of synonymous, nonsynonymous and intergenic mutations was counted for sequenced regions. Second, we simulated 1000 times the expected distribution of mutations in the genome given the previously computed mutational spectra (Remigi *et al.* 2014). This allowed the determination of the expected values of these mutational events under the null hypothesis that mutations are randomly distributed. The simulated dN/dS (nonsynonymous to synonymous substitution rate), dI/dS (intergenic to synonymous substitution rate) and number of mutations in COG functions were then compared to the values observed in the experimental data set.

Results

Short and long cycles increased bacterial fitness on rhizoplane and within nodules

The nine LC lineages (CBM212-derived lines DEF, CBM349-derived lines IJK and CBM356-derived lines PRT) were generated in parallel to the nine SC lineages (CBM212-derived lines ABC, CBM349-derived lines GHI and CBM356-derived lines MNS) (Fig. S1, Supporting information), except that serial ex planta–in planta cycles were twice as long to evaluate the impact of the length of the cycles on the evolution of symbiotic properties.

In each cycle, inoculated bacteria first diffused in the plant culture Jensen medium, then colonized the *Mimosa* rhizoplane and finally entered the root and multiplied within infection threads of newly formed nodules. Nodules were regularly formed all along the plant–bacteria incubation time. In the 42-day LC series, we estimated *ca.* 13.5 days and 28.5 days the mean times bacteria spent ex planta and in planta,

respectively, instead of 7 and 14 days, respectively, for 21-day SC series (Remigi *et al.* 2014). To compare LC and SC evolution, we first evaluated fitness changes in the three successive compartments, the Jensen plant medium, the rhizoplane and the nodules.

To evaluate changes in plant medium and rhizoplane colonization ability, we introduced a constitutive *psbA*-GFP and a *psbA*-mCherry fusion in each of the ancestral and final clones, respectively. Each pair of ancestral-GFP/final-mCherry clones was co-inoculated to *Mimosa pudica* at a ratio of 1:1 and the relative fitness of each evolved clone was estimated by counting the respective number of final and ancestral clones recovered from the plant culture medium and from the rhizoplane at 7 dpi. Less than half of final clones had an increased fitness as compared to their ancestors in the plant culture medium population, and the difference was often low (10%) (Fig. S2, Supporting information). By contrast, except for A16 and P16, final clones of each lineage represented 60–90% of the rhizoplane population (Fig. S2, Supporting information), indicating they have generally increased their ability to colonize the rhizoplane.

To evaluate changes in both extra- and intracellular nodule infection capacity, final clones were individually inoculated to *M. pudica* and the in planta fitness was evaluated at 21 and 42 dpi. The number of bacteria per nodule was estimated by plating dilutions of surface-sterilized and crushed nodules on culture medium and counting the number of colony-forming units (CFUs). All final clones produced one to two more log (10) CFUs than their respective ancestors, a situation already observed for SC clones (Marchetti *et al.* 2014), except for A16 (Fig. 1A). They however still produced at least one log less CFUs than the reference rhizobium strain *Cupriavidus taiwanensis* and a *nifH* mutant of *C. taiwanensis*, except for L16 at 42 dpi (Fig. S3, Supporting information).

No difference could be evidenced between LC and SC final clones regarding fitness changes in the Jensen plant medium, the rhizoplane and the nodules (Table S1, Supporting information). Moreover, none of the final clones fixed nitrogen as evaluated by visual observation of shoots and fresh sections of nodules.

Altogether, this showed that, whatever the selection regime, 16 cycles of ex planta–in planta passages improved the ability of nearly all final clones to colonize the rhizoplane and the nodules, but did not allow acquisition of symbiotic nitrogen fixation.

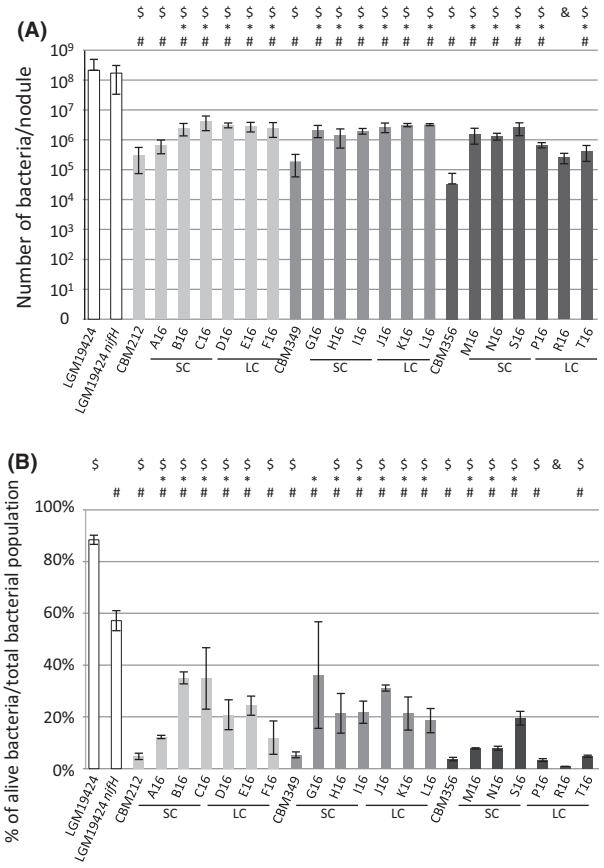

Fig. 1 In planta fitness and persistence of endosymbiotic-evolved clones. *Mimosa pudica* plants were inoculated with *Cupriavidus taiwanensis* wild type (LMG19424), its *nifH* mutant or evolved clones and nodules were recovered at 21 dpi. (A) Nodule bacteria were counted after plating. (B) Total bacteria recovered from nodules were stained with SYTO9 and PI and analysed on a flow cytometer for viability. Results are reported as percentage of Syto9-stained bacteria of the total bacterial population. Six plants (A) or 15–20 nodules (B) were analysed in each experiment, except for R16 that nodulates poorly, and for which, only five or six nodules were analysed for fitness or persistence, respectively. The mean ± SD of three independent experiments is represented. *, $ and # indicate significant difference with the ancestor of the lineage, the *C. taiwanensis* wild-type strain and the *C. taiwanensis nifH* mutant, respectively ($P < 0.05$; Student's *t*-test). & indicates no statistical analysis applicable because not enough points. The CBM212-, CBM349- and CBM356-derived lineages are in three different shades of grey.

Short and long regimes similarly improved intracellular infection

Among the three spontaneous nodulating variants of *Ralstonia* GMI1000pRalta, obtained in our experimental system, two of them, CBM212 and CBM349, were able to intracellularly infect *Mimosa* nodules, although rudimentarily as compared to the *M. pudica* symbiont *C. taiwanensis*. This capacity was dramatically improved in five (B, C, G, H and I) of the six SC lineages, concomitantly to a decrease in plant defence reactions within nodules (Marchetti *et al.* 2014).

To evaluate how the long selection regime impacted on the improvement of intracellular infection, we

analysed three symbiotic traits that account for the quality of intracellular infection, that is the size of the intracellularly infected zone, the size of the necrotic zone and the persistence of nodule bacteria at 21 dpi.

Intracellularly infected and necrotic areas were measured on sections of nodules (see 'Materials and methods') collected 21 days after *M. pudica* inoculation with the final clones of the D, E, F, J, K and L long lineages (Fig. 2A,B). The CBM212-derived final clones D16, E16 and F16 and the CBM349-derived final clone K16 exhibited significantly improved nodule intracellular colonization and decreased plant defence reactions as compared to their relative ancestor. The CBM349-derived final clones J16 and L16 formed nodules with decreased necrosis, but their intracellular colonization was statistically not improved (Fig. 2A,B). At a global scale, the level of infection and necrosis of CBM212- and CBM349-derived final clones obtained via long cycles showed no significant difference as compared to CBM212- and CBM349-derived clones obtained via short cycles (Table S2, Supporting information).

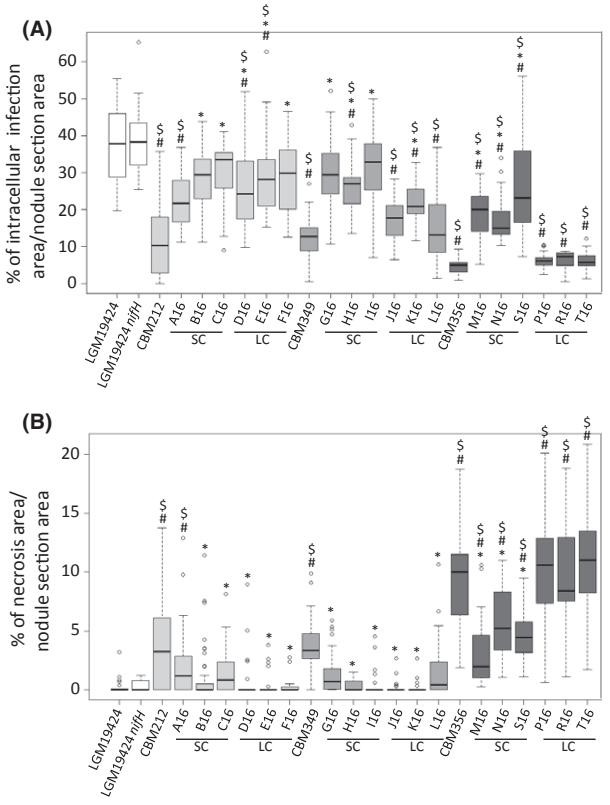

Fig. 2 Infection phenotyping of evolved clones derived from short and long regimes. *Mimosa* nodules formed by ancestors, evolved clones, *Cupriavidus taiwanensis* or a *C. taiwanensis nifH* mutant were analysed for infection and necrosis at 21 dpi. The intracellular infection and the necrosis zones were measured on nodule sections using the IMAGE-PRO software and divided by the total nodule surface. Box plots represent the percentage of nodule infection (A) or necrosis (B) evaluated from 12 to 48 nodules per strain in two or three independent experiments. The central rectangle spans the first quartile to the third quartile (i.e. the interquartile range or IQR), the segment inside the rectangle shows the median, and whiskers above and below the box show minimum and maximum in the absence of suspected outlying data. Data for *C. taiwanensis*, *C. taiwanensis nifH* and final clones of the A, B, C, G, H, I, M, N and S lineages were from (Marchetti *et al.* 2014). *, # and $ indicate statistically significant differences with the respective ancestral strain, the reference strain *C. taiwanensis* and the *C. taiwanensis nifH* mutant, respectively ($P < 0.05$; Kruskal–Wallis test). The CBM212-, CBM349- and CBM356-derived lineages are in three different shades of grey.

Bacterial persistence within nodules was evaluated by analysing the viability of bacteria recovered from nodules at 21 dpi, including both intracellular and intercellular bacteria, using a live/dead staining procedure (see 'Materials and methods'). Except for F16, the percentage of alive bacteria was significantly higher for final evolved clones than for their relative ancestors (Fig. 1B). No significant difference between clones obtained via long and short regimes could be observed (Table S2, Supporting information). However, none of the final evolved clone exhibited a persistence comparable to that of the reference strain *C. taiwanensis* or of its *nifH* mutant, except G16 that was not found significantly different from *C. taiwanensis nifH*.

Overall, long and short final clones were not significantly different, indicating that once infection has been activated, long and short cycles act similarly.

The long regime favoured extracellular infection when intracellular infection is not already activated

The third nodulating ancestor, CBM356, was not capable of intracellular infection (Marchetti *et al.* 2010). This capacity was however further acquired in the M, N and S lineages derived via short cycles (Guan *et al.* 2013). To evaluate whether the selection regime of long cycles allowed the acquisition of intracellular infection, we measured the size of the intracellularly infected and necrotic zones, as well as the persistence of nodule bacteria in nodules formed by CBM356-derived final clones at 21 dpi.

The size of the intracellular infection area of CBM356-derived LC clones P16, R16 and T16 was found similar to that of CBM356, indicating that these clones did not acquire intracellular infection capacity (Fig. 2A). These clones exhibited a necrotic dark brown zone of similar size than CBM356, indicating that they induce plant defence reactions at the same level (Fig. 2B). Moreover, they did not show increased persistence of nodule bacteria as compared to CBM356. P16, R16 and T16 thus behaved differently from CBM356-derived SC final clones M16, N16 and S16, which were capable of

Mimosa nodule cell infection, formed significantly decreased necrotic zones within nodules and exhibited increased endosymbiotic persistence as compared to their ancestor (Guan *et al.* 2013) (Figs 1B and 2A,B). These results were surprising as nodules formed by the P16, T16 and R16 clones produced ca. one more log CFUs than their ancestor CBM356 (Fig. 1A). We thus hypothesized that these clones improved their capacity to intercellularly infect nodules. The level of extracellular infection on sections of nodules formed by P16, R16 and T16 bearing a constitutively expressed *LacZ* fusion was measured using the HIS method. This confirmed that P16 and T16 clones have a significantly higher extracellular infection capacity than their ancestor (Fig. 3B–F). Moreover, co-inoculation experiments showed that P16 and T16 were more fit in planta than their CBM356 ancestor (Fig. 3A). These analyses were not performed on R16, as it formed very few nodules on *M. pudica*.

Altogether, these results showed that the long regime did not favour the activation of intracellular infection capacity, but instead improved extracellular infection.

Mutations activating intracellular infection were fixed in CBM356-derived long lines but countered by additional genomic changes

It is possible that during laboratory evolution, no adaptive mutation for intracellular infection occurred in the bacterial population at infection sites, resulting in the lack of intracellular infection activation. Alternatively, adaptive mutations could have arisen but not been fixed in the long-cycle selection regime, or their effect further suppressed by additional mutations. To evaluate these three possibilities, we analysed the infection phenotype of a few intermediate clones of the P, R and T lineages. We found that at least one clone of the R line, R11, was able to intracellularly infect nodule cells, and

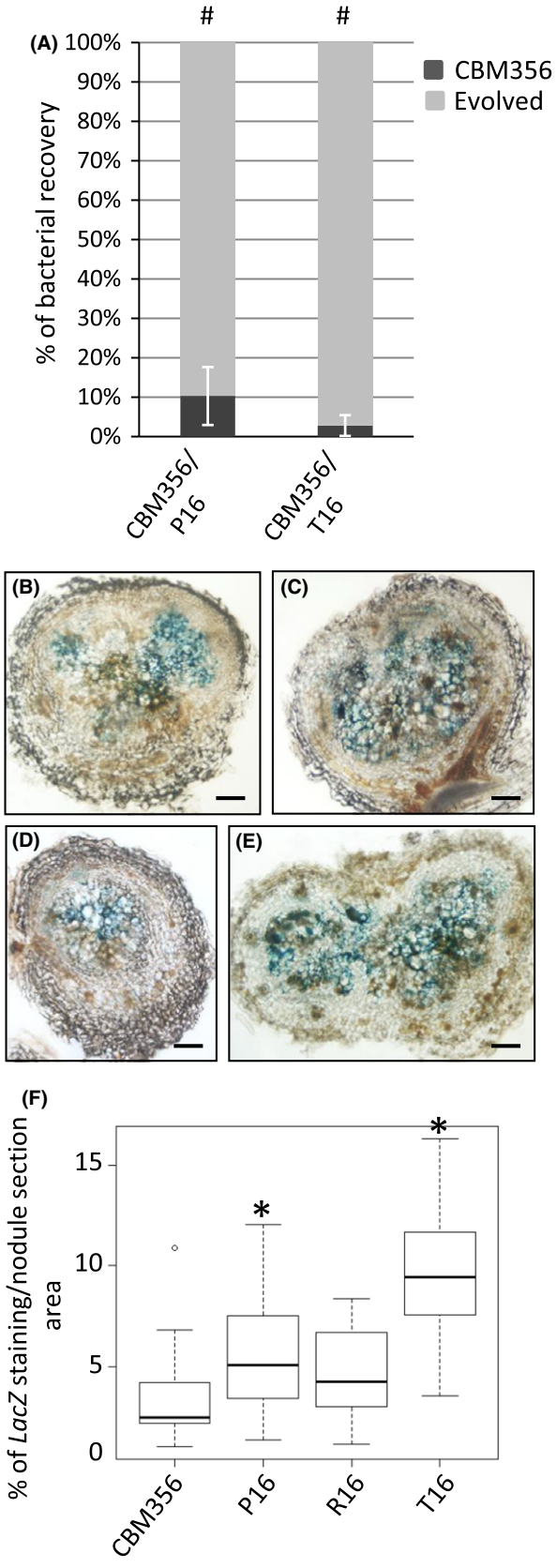

Fig. 3 In planta relative fitness and extracellular infection of CBM356-derived final clones of the LC regime. (A) *Mimosa pudica* plantlets were co-inoculated with pairs of strains at a 1:1 ratio. Nodules were harvested at 21 dpi, and the number of nodule bacteria was evaluated by plating. Two experiments of 20 plants each were performed. (B–E) Nodules formed by the CBM356 ancestor (B) or the evolved clones P16 (C), R16 (D) and T16 (E) expressing a constitutive *lacZ* fusion were analysed for extracellular infection at 21 dpi. Nodule sections were stained with X-Gal for microscopic visualization (B–E) and quantification analysis of six to 25 nodules (F). The mean ± SD is represented. # indicates statistically significant differences between the two bacterial populations ($P < 0.05$, Student's *t*-test). * indicates statistically significant differences with the CBM356 ancestor ($P < 0.05$; Kruskal–Wallis test). Scale bar = 100 μm.

induced significantly decreased nodule necrosis (Fig. 4). This indicates that intracellular infection capacity arose in the R lineage but has not been fixed during laboratory evolution.

To search for potential adaptive mutations, we resequenced the final clones P16, R16 and T16, as well as the intermediate clone R11 and sequence data were mapped to the ancestral reference genome (6.37 Mb) based on the known genome of *Ralstonia solanacearum* GMI1000 (Salanoubat *et al.* 2002) and *C. taiwanensis* LMG19424 (Gonzalez *et al.* 2006). In all clones, we found a mutation affecting the *prhAIRJhrpG* regulatory pathway. Mutations altering this regulatory cascade were previously shown to allow intracellular infection (Marchetti *et al.* 2010; Guan *et al.* 2013). The master virulence regulator *hrpG* (Poueymiro & Genin 2009) was altered by a nonsynonymous mutation leading to the E214K and the A179V modification of the protein in P16 and R11/R16, respectively. A nonsynonymous mutation (R203C) affecting the *prhA* gene encoding a bacterial sensor of plant cell contact (Aldon *et al.* 2000) was identified in T16. To evaluate the possible role of the *hrpG*A179V mutation in intracellular infection, we reconstructed this mutation in the nodulating CBM356 ancestor. In contrast to CBM356, its *hrpG*A179V mutant induced nodules that exhibited rudimentary cell infection (Fig. 4). The sizes of the intracellularly infected and necrotic areas were comparable to those observed for R11, indicating that the *hrpG*A179V mutation was adaptive for intracellular infection (Fig. 4G,H). Co-inoculation experiments confirmed that the CBM356 strain carrying the *hrpG* A179V mutation (CBM356 *hrpG*) was more fit in planta than CBM356 at 21 dpi (Fig. 4F). However, R16 was as expected less fit than CBM356 *hrpG*A179V because of its poorly nodulation capacity. These results suggested the occurrence in R16 of

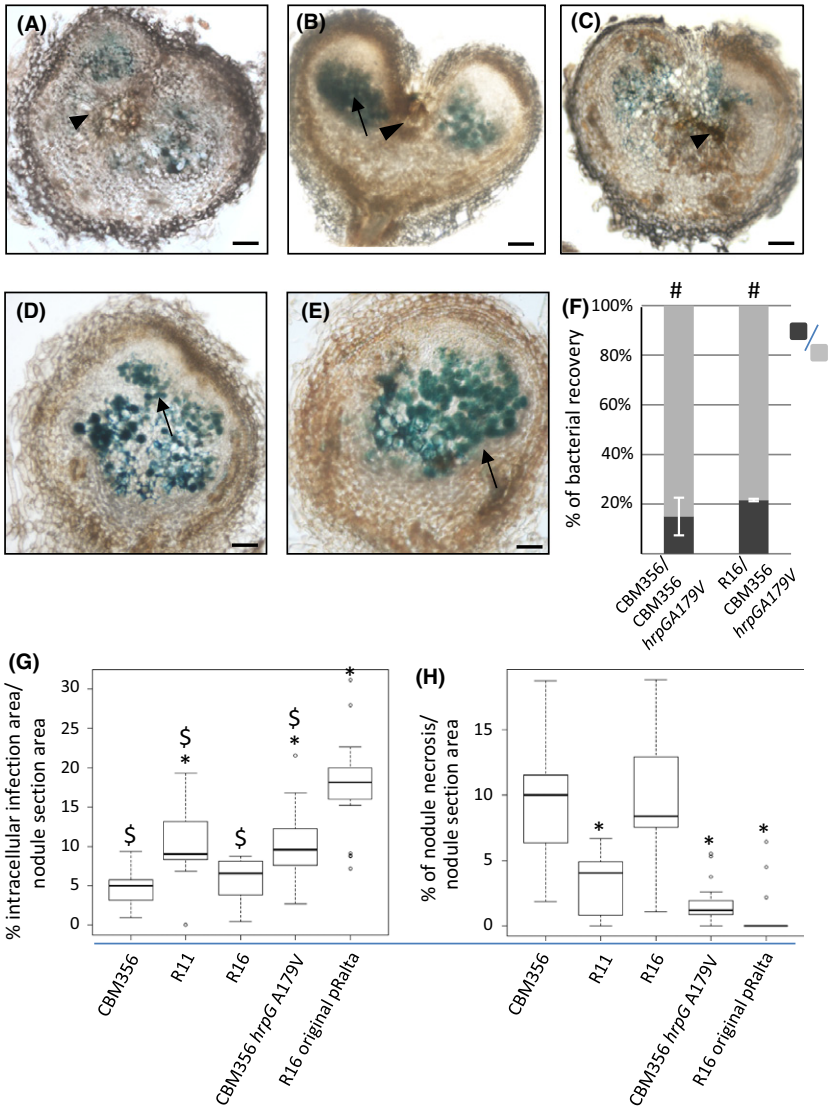

Fig. 4 Acquisition of intracellular infection in the R line. Sections of *Mimosa* nodules formed by CBM356 (A), R11 (B), R16 (C), CBM356 *hrpG*A179V (D) and R16 original pRalta (E) constitutively expressing a *lacZ* fusion were analysed for infection and necrosis at 21 dpi. (F) Relative fitness of CBM356 *hrpG* A179V measured on *Mimosa* nodules recovered at 21 dpi after co-inoculation with CBM356 or R16 at a ration 1:1. Three experiments for each competition were realized. Intracellular infection (G) and necrosis (H) quantification were performed on sections obtained from 12 to 23 nodules formed by CBM356, R11, R16, CBM356*hrpG*A179V and R16 original pRalta at 21 dpi. Arrows and arrowheads indicate infected cells and necrotic zones, respectively. The mean ± SD of three independent experiments is represented. # indicates statistically significant differences between the two bacterial populations ($P < 0.05$, Student's *t*-test).* and $ indicate significant differences with the CBM356 ancestor and the R16 original pRalta strain, respectively ($P < 0.05$; Kruskal–Wallis test). Scale bar = 100 μm.

additional changes that countered the adaptive effect of *hrpG*A179V. Indeed, changing the evolved pRalta of R16 by the original pRalta restored the CBM356 *hrpG*A179V phenotype, indicating that genomic modifications in pRalta were responsible for the suppression of the capacity for intracellular infection (Fig. 4G,H).

Long-cycle lineages accumulated more mutations than short-cycle lineages

The plant culture medium environment was shown to induce transient hypermutagenesis in the chimeric *Ralstonia* (Remigi *et al.* 2014). As bacteria spent more time in this environment in the long cycles, we expected to observe the accumulation of more mutations in these clones than those evolved through short cycles. We thus sequenced the D16, E16, F16, J16, K16 and L16 final clones and compared the number of their genomic changes with those of the previously sequenced SC final clones (Remigi *et al.* 2014). We identified between 56 and 138 point mutations (SNPs, indels) scattered in the genomes of the clones from the long cycles that were absent from the chimeric GMI1000pRalta ancestor. Hence, clones evolved using the long selection regime harboured 1.5 times more mutations than short regime-evolved clones (Table 2, Student's *t*-test, *P*-value = 0.006).

We then enquired on the differences between short and long cycles regarding the mutational patterns and ensuing natural selection. The long-evolved clones showed no significant differences in terms of synonymous/nonsynonymous substitution rates (d*N*/d*S*), intergenic/intergenic substitution rates (d*I*/d*S*) and transitions/transversions rates (ts/tv) (all Student's *t*-tests, *P*-value > 0.05) (Table 1). Chromosomes 1 and 2, but not the symbiotic plasmid, showed a strong signal of purifying selection (excess of synonymous over nonsynonymous mutations), as already observed for short regime-evolved clones (Remigi *et al.* 2014). The d*I*/d*S* was significantly higher than expected on the two chromosomes of the long cycles (Table 2), a feature observed for chromosome 2 in short-evolved clones. Further work will be necessary to assess whether this reflects positive selection for mutations in regulatory regions.

Discussion

Use of experimental evolution to analyse the evolutionary mechanisms leading to symbiosis with legumes requires developing an appropriate experimental setting for the evolution of symbiotic traits. Rhizobial symbiosis is a complex process involving many successive stages, including rhizoplane colonization, root entry, nodule organogenesis, nodule cell infection, bacteroid persistence and nitrogen fixation, which may not be under the same selection pressures and control mechanisms. Typically, plant hosts select the most efficiently nodulating rhizospheric bacteria before the establishment of the symbiosis (partner

Table 1 Analysis of mutations in SC and LC final clones

Regime of selection	Clones	Number of different SNPs/indels	Syn/Nonsyn	Genic/Intergenic	Ts/Tv
SC	A16	76/0	24/42	66/10	66/10
	B16	77/0	26/46	71/6	73/4
	C15	126/1	40/72	113/14	114/12
	G16	73/0	30/35	64/9	67/6
	H16	62/0	22/36	56/6	54/8
	I16	97/1	39/48	84/14	92/5
	M16	39/1	15/19	34/6	32/7
	N16	51/1	19/25	42/10	45/6
	S16	48/0	18/23	39/9	45/3
	Mean	72.11/0.44	25.89/38.44	63.22/9.33	65.33/6.78
LC	D16	117/2	46/59	106/13	107/10
	E16	125/0	45/68	113/12	103/22
	F16	115/0	36/62	98/17	103/12
	J16	92/1	31/48	79/14	84/8
	K16	136/2	56/61	118/20	125/11
	L16	118/0	46/57	102/16	108/10
	P16	56/0	20/28	47/9	47/9
	R16	82/1	30/37	67/16	76/6
	T16	119/0	53/51	102/17	104/15
	Mean	106.67/0.67	40.33/52.33	92.44/14.89	95.22/11.44

Syn, synonymous; Nonsyn, nonsynonymous; Ts, transition; Tv, transversion.

Table 2 d*N*/d*S* and d*I*/d*S* ratios.

		d*N*/d*S**			d*I*/d*S*†		
Selection regime	Replicon	Observed	Expected	*P*-value	Observed	Expected	*P*-value
SC	Chromosome 1	0.431	0.720	0.001	0.586	0.784	0.218
	Chromosome 2	0.508	0.735	0.011	1.334	0.794	0.044
	pRalta	0.669	0.617	0.305	0.660	0.710	0.464
LC	Chromosome 1	0.398	0.707	0.001	1.587	0.769	0.001
	Chromosome 2	0.384	0.708	0.001	2.636	0.758	0.001
	pRalta	0.590	0.592	0.475	0.741	0.674	0.660

*Ratio of the number of nonsynonymous substitutions per nonsynonymous site to the number of synonymous substitutions per synonymous sit.
†Ratio of the number of intergenic substitutions per intergenic site to the number of synonymous substitutions per synonymous site.

choice) (Ling *et al.* 2013) and punish poorly nitrogen-fixing endosymbionts after the establishment of symbiosis (host sanctions) (Kiers *et al.* 2003). We previously demonstrated that 21-day cycles of ex planta–in planta (*Mimosa*) passages select for chimeric *Ralstonia* exhibiting increased nodulation competitiveness that was accompanied by the activation or improvement of intracellular infection capacity, a prerequisite for symbiotic nitrogen fixation (Guan *et al.* 2013; Marchetti *et al.* 2014). Here, we showed that variation in the time span of the plant–bacteria coculture cycles may lead to divergent evolutionary patterns in terms of nodule endosymbiosis. Short cycles led to the evolution of the capacity for intracellular infection, an exclusive trait of mutualistic rhizobia, and long cycles led to parasitic intercellular infection. This shows that experimental design may have an essential role in shaping the evolution of biotic interactions.

Whatever the selection regime, that is 21- or 42-day cycles, 16 cycles of evolution drastically improved the capacity of bacteria to colonize the *Mimosa* rhizoplane and nodules. The observed increase in rhizoplane colonization is in accordance with the recent observation that the rhizoplane plays a selective gating role (Edwards *et al.* 2015). Gain in in planta fitness results from gain either in nodulation competitiveness or in nodule colonization or both and is directly linked to the mode of selection. Indeed, in each cycle, bacteria used as inoculum were isolated from root nodules, that is where bacteria outcompeted other clonemates for nodulation. Moreover, bacteria that have massively multiplied inside nodules at 21 or 42 dpi are better represented in the collected nodule populations serving as inocula and thus have more chance to nodulate in the next cycle. The ultimate stage of symbiotic nitrogen fixation was not gained in any line, possibly because bacteroid persistence remains limited within the allotted time.

Improved nodule colonization may be due to either a better extracellular infection, or a better intracellular infection of nodules or both. Notably, although they induce the formation of indeterminate nodules, *C. taiwanensis* symbionts of *Mimosa* spp. are not terminally differentiated and at least a part of bacteroids recovered from nodules in each cycle can resume growth and form nodules on a new set of plants (Marchetti *et al.* 2011). In lines derived from the two ancestors that are capable of rudimentary intracellular infection, both SC and LC regimes lead to similar improvement of intracellular infection quantity and quality. On the other hand, SC and LC regimes induced divergent endosymbiotic phenotypes on lines derived from the extracellular infectious ancestor CBM356. While the three SC final clones acquired nodule cell infection capacity, none of the LC final clones got this ability. By contrast, these clones exhibited an enhanced infection of intercellular spaces of nodules, indicating that the long-cycle regime favoured this mode of infection in these lines. An attempt of explanation is that bacteroids are more persistent at 21 dpi than at 42 dpi. When beneficial mutations for intracellular infection arise, experimental setting may differently act on this trait. At 21 dpi, infectious protosymbionts might be persistent enough to outnumber extracellular bacteria, and thus, intracellular infection would be favoured in SC. At 42 dpi, bacteroids are degenerated and only extracellular bacteria would survive, thus favouring extracellular infection. In our system, extracellular infection is generally associated with the presence of necrotic zones within nodules, indicative of a plant immune response. Whereas intercellular infection has been recently described for endophytic bacteria that coexist with rhizobia within nodule tissues (Zgadzaj *et al.* 2015), extracellular infection by nodule bacteria is very rare in nature, and has been observed only when appropriate partners are absent (Gehlot *et al.* 2013). This could be

due to the fact that optimal intracellular infection allows very large amplification of rhizobia, and thus, intracellularly infectious rhizobia are expected to rapidly outcompete rhizobia only present in intercellular spaces in natura. Further analyses should identify extracellular infection-adaptive mutations and reveal which biological modifications, for example avoidance of plant defences or better use of plant substrates, are responsible for the enhancement of this divergent symbiotic evolution.

Interestingly, at least one intermediate clone of the R line, R11, exhibited intracellular infection capacity. Moreover, the three LC CBM356-derived final clones harbour a mutation in the *prhAIRJhrpG* regulatory cascade, the alteration of which has previously been shown to derepress intracellular infection in chimeric *Ralstonia* (Marchetti *et al.* 2010; Guan *et al.* 2013). We indeed showed that the *hrpG* mutation in R11, which is conserved in R16, is adaptive for nodule cell infection, converting CBM356 into an intracellularly infectious clone. Replacing the evolved pRalta of R16 by the original pRalta restored the intracellular infectious phenotype, indicating that the pRalta harbours mutation(s) that countered the effect of the *hrpG* mutation. We speculate that mutations in the *prhARIJhrpG* cascade arose and were fixed along time in all CBM356-derived lines as they improve nodulation competitiveness and allow rudimentary intracellular infection, as previously demonstrated (Guan *et al.* 2013), but their intracellular infection-adaptive effect was suppressed by subsequent genomic changes favoured in the LC context, likely increasing extracellular infection capacity. These *prhARIJhrpG* mutations could have been maintained for their impact on nodulation competitiveness. Hence, incapacity for intracellular infection resulted from natural selection and not from lack of appropriate mutations. Further studies should identify the pRalta-suppressive mutation(s) and their role in extracellular infection.

The analysis of mutational events showed that clones evolved *via* the long regime of selection harboured a significant (50%) excess of point mutations as compared to short regime. Previous work showed that bacteria were submitted to transient plasmid *imuABC*-based hypermutagenesis during laboratory evolution and accumulated mutations ex planta (Remigi *et al.* 2014). We hypothesize that the increase in mutation number was mainly due to a longer period spent ex planta. Yet, the characteristics of the genome evolution were not impacted by the selection regime. Both regimes had a strong signature of purifying selection, suggesting that most deleterious nonsynonymous mutations were removed from populations (Yang & Bielawski 2000) and a significantly higher dI/dS than expected, suggesting that modification in gene expression was selected during the laboratory evolution. In both regimes, the second chromosome had higher dN/dS and dI/dS, likely because it encodes for genes involved in biological functions that might be inactivated, modulated or recruited for symbiosis, for example virulence, flagellum and exopolysaccharide synthesis, primary metabolism and adaptation to environmental conditions.

The importance of microbiome in animal and plant health and fitness is increasingly recognized, and has led to international initiatives to further explore and exploit the capabilities of Earth's microbial ecosystems (Alivisatos *et al.* 2015; Dubilier *et al.* 2015). Beyond identifying microbes, microbial communities and the mechanisms by which they interact with higher organisms, the development of tools to manipulate the microbiome in situ or in the laboratory (Mueller & Sachs 2015; Ravi *et al.* 2016) promises groundbreaking innovations in the agriculture, health and green industry. An emerging trend in plant microbiology is to artificially select microbiomes for traits of interest indirectly through the host (Mueller & Sachs 2015). Host-mediated selection, including experimental evolution approaches, involves selection by the host of the most-adapted microbial communities. Our work highlights the importance of the selection regime to shape the desired traits.

Acknowledgements

We are grateful to Jacques Batut for helpful comments on the manuscript. This work was supported by funds from the French National Research Agency (ANR-12-ADAP-0014-01), the French Laboratory of Excellence project 'TULIP' (ANR-10-LABX-41; ANR-11-IDEX-0002-02), the France Génomique National Infrastructure, funded as part of 'Investissement d'avenir' programme managed by the French National Research Agency (ANR-10-INBS-09) and by a European Research Council starting grant [EVOMOBILOME n°281605] to EPCR. CC was supported by the French National Research Agency (ANR-12-ADAP-0014-01).

References

Aldon D, Brito B, Boucher C, Genin S (2000) A bacterial sensor of plant cell contact controls the transcriptional induction of *Ralstonia solanacearum* pathogenicity genes. *EMBO Journal*, **19**, 2304–2314.

Alivisatos AP, Blaser MJ, Brodie EL *et al.* (2015) A unified initiative to harness Earth's microbiomes. *Science*, **350**, 507–508.

Barrick JE, Yu DS, Yoon SH *et al.* (2009) Genome evolution and adaptation in a long-term experiment with *Escherichia coli*. *Nature*, **461**, 1243–1247.

Boucher CA, Barberis PA, Trigalet AP, Demery DA (1985) Transposon mutagenesis of *Pseudomonas solanacearum* –

isolation of TN5-induced avirulent mutants. *Journal of General Microbiology*, **131**, 2449–2457.

Brockhurst MA, Koskella B (2013) Experimental coevolution of species interactions. *Trends in Ecology & Evolution*, **28**, 367–375.

Brockhurst MA, Colegrave N, Rozen DE (2011) Next-generation sequencing as a tool to study microbial evolution. *Molecular Ecology*, **20**, 972–980.

Buckling A, Maclean RC, Brockhurst MA, Colegrave N (2009) The Beagle in a bottle. *Nature*, **457**, 824–829.

Charpentier M, Oldroyd G (2010) How close are we to nitrogen-fixing cereals? *Current Opinion in Plant Biology*, **13**, 556–564.

Chrostek E, Teixeira L (2015) Mutualism breakdown by amplification of Wolbachia genes. *PLos Biology*, **13**, e1002065. doi: 10.1371/journal.pbio.1002065.

Dalia AB, McDonough E, Camilli A (2014) Multiplex genome editing by natural transformation. *Proceedings of the National Academy of Sciences of the United States of America*, **111**, 8937–8942.

Dubilier N, McFall-Ngai M, Zhao L (2015) Create a global microbiome effort. *Nature*, **526**, 631–634.

Edwards J, Johnson C, Santos-Medellin C *et al.* (2015) Structure, variation, and assembly of the root-associated microbiomes of rice. *Proceedings of the National Academy of Sciences of the United States of America*, **112**, E911–E920.

Elena S, Lenski R (2003) Evolution experiments with microorganisms: the dynamics and genetic bases of adaptation. *Nature Reviews Genetics*, **4**, 457–469.

Gehlot HS, Tak N, Kaushik M *et al.* (2013) An invasive *Mimosa* in India does not adopt the symbiont of its native relatives. *Annals of Botany*, **1**, 179–196.

Gibson KE, Kobayashi H, Walker GC (2008) Molecular determinants of a symbiotic chronic infection. *Annual Review of Genetics*, **42**, 413–441.

Gonzalez V, Santamaria RI, Bustos P *et al.* (2006) The partitioned *Rhizobium etli* genome: genetic and metabolic redundancy in seven interacting replicons. *Proceedings of the National Academy of Sciences of the United States of America*, **103**, 3834–3839.

Guan SH, Gris C, Cruveiller S *et al.* (2013) Experimental evolution of nodule intracellular infection in legume symbionts. *ISME Journal*, **7**, 1367–1377.

Guidot A, Jiang W, Ferdy J-B *et al.* (2014) Multihost experimental evolution of the pathogen *Ralstonia solanacearum* unveils genes involved in adaptation to plants. *Molecular Biology and Evolution*, **31**, 2913–2928.

Hirsch AM, Wilson KJ, Jones JDG *et al.* (1984) *Rhizobium meliloti* nodulation genes allow *Agrobacterium tumefaciens* and *Escherichia coli* to form pseudondules on *alpha-alpha*. *Journal of Bacteriology*, **158**, 1133–1143.

Jackson RW, Johnson LJ, Clarke SR, Arnold DL (2011) Bacterial pathogen evolution: breaking news. *Trends in Genetics*, **27**, 32–40.

Kiers E, Rousseau R, West S, Denison R (2003) Host sanctions and the legume-rhizobium mutualism. *Nature*, **425**, 78–81.

Ling J, Zheng H, Katzianer DS *et al.* (2013) Applying reversible mutations of nodulation and nitrogen-fixation genes to study social cheating in *Rhizobium etli*-legume interaction. *PLoS One*, **8**, e70138. doi: 10.1371/journal.pone.0070138.

Long A, Liti G, Luptak A, Tenaillon O (2015) Elucidating the molecular architecture of adaptation via evolve and resequence experiments. *Nature Reviews Genetics*, **16**, 567–582.

MacLean RC, Hall AR, Perron GG, Buckling A (2010) The population genetics of antibiotic resistance: integrating molecular mechanisms and treatment contexts. *Nature Reviews Genetics*, **11**, 405–414.

Marchetti M, Capela D, Glew M *et al.* (2010) Experimental evolution of a plant pathogen into a legume symbiont. *PLos Biology*, **8**, 1000280. doi: 10.1371/journal.pbio.1000280.

Marchetti M, Catrice O, Batut J, Masson-Boivin C (2011) *Cupriavidus taiwanensis* bacteroids in *Mimosa pudica* indeterminate nodules are not terminally differentiated. *Applied and Environmental Microbiology*, **77**, 2161–2164.

Marchetti M, Jauneau A, Capela D *et al.* (2014) Shaping bacterial symbiosis with legumes by experimental evolution. *Molecular Plant-Microbe Interactions*, **27**, 956–964.

Masson-Boivin C, Giraud E, Perret X, Batut J (2009) Establishing nitrogen-fixing symbiosis with legumes: how many rhizobium recipes? *Trends in Microbiology*, **17**, 458–466.

Monteiro F, Solé M, van Dijk I, Valls M (2012) A chromosomal insertion toolbox for promoter probing, mutant complementation, and pathogenicity studies in *Ralstonia solanacearum*. *Molecular Plant-Microbe Interactions*, **25**, 557–568.

Mueller UG, Sachs JL (2015) Engineering microbiomes to improve plant and animal health. *Trends in Microbiology*, **23**, 606–617.

Oldroyd GED, Murray JD, Poole PS, Downie JA (2011) The rules of engagement in the legume-rhizobial symbiosis. In: *Annual Review Genetics*, **45**, 119–144.

Paterson S, Vogwill T, Buckling A *et al.* (2010) Antagonistic coevolution accelerates molecular evolution. *Nature*, **464**, 275–278.

Poueymiro M, Genin S (2009) Secreted proteins from *Ralstonia solanacearum*: a hundred tricks to kill a plant. *Current Opinion in Microbiology*, **12**, 44–52.

Ravi U, Sheth VC, Chen Sway P, Wang Harris H (2016) Manipulating bacterial communities by *in situ* microbiome engineering. *Trends in Genetics*, **32**, 189–250.

Remigi P, Capela D, Clerissi C *et al.* (2014) Transient hypermutagenesis accelerates the evolution of legume endosymbionts following horizontal gene transfer. *PLos Biology*, **12**, e1001942. doi: 10.1371/journal.pbio.1001942.

Remigi P, Zhu J, Young JPW, Masson-Boivin C (2016) Symbiosis within symbiosis: evolving nitrogen-fixing legume symbionts. *Trends in Microbiology*, **24**, 63–75.

Salanoubat M, Genin S, Artiguenave F *et al.* (2002) Genome sequence of the plant pathogen *Ralstonia solanacearum*. *Nature*, **415**, 497–502.

Scanlan PD, Hall AR, Lopez-Pascua LDC, Buckling A (2011) Genetic basis of infectivity evolution in a bacteriophage. *Molecular Ecology*, **20**, 981–989.

Sullivan JT, Patrick HN, Lowther WL, Scott DB, Ronson CW (1995) Nodulation strains of *Rhizobium loti* arise through chromosomal symbiotic gene-transfer in the environment. *Proceedings of the National Academy of Sciences of the United States of America*, **92**, 8985–8989.

Tian CF, Zhou YJ, Zhang YM *et al.* (2012) Comparative genomics of rhizobia nodulating soybean suggests extensive recruitment of lineage-specific genes in adaptations.

Proceedings of the National Academy of Sciences of the United States of America, **109**, 8629–8634.

Yang ZH, Bielawski JP (2000) Statistical methods for detecting molecular adaptation. *Trend in Ecology and Evolution*, **15**, 496–503.

Yang L, Jelsbak L, Marvig RL *et al*. (2011) Evolutionary dynamics of bacteria in a human host environment. *Proceedings of the National Academy of Sciences of the United States of America*, **108**, 7481–7486.

Zgadzaj R, James EK, Kelly S *et al*. (2015) A legume genetic framework controls infection of nodules by symbiotic and endophytic bacteria. *PLos Genetics*, **11**, e1005280. doi: 10.1371/journal.pgen.1005280

M.M. and C.B.M. conceived and designed the experiments. C.C., Y.Y., D.C., M.M. and C.G. performed the experiments. C.C., D.C., M.M., A.J. and C.M.B. analysed the data. E.R. shared analysis tools. S.C. contributed analysis tools. C.M.B. wrote the manuscript.

Data accessibility

The complete collections of events generated for all the clones from this study are available on the Microscope platform (https://www.genoscope.cns.fr/agc/microscope/expdata/evoProject.php, SYMPA tag).

Supporting information

Additional supporting information may be found in the online version of this article.

Fig. S1 Lab-evolution of symbiotically-improved *Ralstonia*.

Fig. S2 Plant culture medium and rhizoplane relative fitness of evolved clones versus their respective ancestor.

Fig. S3 *In planta* relative fitness of evolved clones at 42 dpi.

Table S1 Comparison of all SC and LC final clones.

Table S2 Comparison of final clones of the CBM212- and CBM349-derived SC and LC lineages.

Table S3 Strains and plasmids used in this study.

Table S4 Primers used in this study.